SUPPORTING INFORMATION:

Ionizable lipid nanoparticles for therapeutic base editing of congenital brain disease

Rohan Palanki[**1,2], Sourav K Bose[**2], Apeksha Dave[2], Brandon M. White[2], Cara Berkowitz[2], Valerie Luks[2], Fazeela Yaqoob[9], Emily Han[1], Kelsey L Swingle[1], Pallavi Menon[2], Emily Hodgson[2], Arijit Biswas[10], Margaret M Billingsley[1], Li Li[6], Fan Yiping[10], Marco Carpenter[2], Alexandra Trokhan[2], Julie Yeo[10], Nuryanti Johana[10], Tan Yi Wan[10], Mohamad-Gabriel Alameh[3], Frederick Chris Bennett[9], Phillip B. Storm[12], Rajan Jain[3,6], Jerry Chan[10,11], Drew Weissman[3], Michael J. Mitchell[*1,4,5,6,7], William H. Peranteau[*2,8]

**Equal contribution

[*]Co-corresponding authors: (M.J.M.) mjmitch@seas.upenn.edu; (W.H.P.) peranteauw@chop.edu

[1]Department of Bioengineering, University of Pennsylvania, Philadelphia, PA 19104, USA.

[2]Center for Fetal Research, Children's Hospital of Philadelphia, Philadelphia, PA 19104, USA.

[3]Department of Medicine, Perelman School of Medicine, University of Pennsylvania, Philadelphia, PA 19104, USA.

[4]Abramson Cancer Center, Perelman School of Medicine, University of Pennsylvania, Philadelphia, PA 19104, USA.

[5]Institute for Immunology, Perelman School of Medicine, University of Pennsylvania, Philadelphia, PA 19104, USA.

[6]Cardiovascular Institute, Perelman School of Medicine, University of Pennsylvania, Philadelphia, PA 19104, USA.

[7]Institute for Regenerative Medicine, Perelman School of Medicine, Philadelphia, PA 19104, USA.

[8]Division of General, Thoracic, and Fetal Surgery, Children's Hospital of Philadelphia, PA, USA.

[9]Department of Psychiatry, Perelman School of Medicine, University of Pennsylvania, Philadelphia, PA 19104, USA.

[10]Duke-NUS Graduate Medical School, Singapore, 169547, SG.

[11]Department of Reproductive Medicine, KK Women's and Children's Hospital, Singapore, 229899, SG.

[12]Division of Neurosurgery, Children's Hospital of Philadelphia, PA 19104, USA.

	Size (nm)	PDI	Encapsulation Efficiency (%)	pK_a	Zeta Potential (mV)
A1	128	0.094	84.2	6.81	8.43
A2	68	0.103	79.9	5.57	2.99
A3	82	0.113	83.5	5.97	4.55
A4	102	0.075	97.0	6.76	11.1
B1	83	0.109	93.4	7.14	3.12
B2	107	0.146	85.1	5.79	5.89
B3	80	0.154	88.1	5.94	10.4
B4	130	0.064	90.2	6.60	15.6
C1	71	0.116	96.6	6.87	2.57
C2	107	0.138	91.1	5.83	7.89
C3	88	0.043	92.0	5.05	9.78
C4	95	0.087	97.6	6.01	2.43

Table S1: Physiochemical properties of LNP library including size, polydispersity index (PDI), encapsulation efficiency, pK_a, and zeta potential.

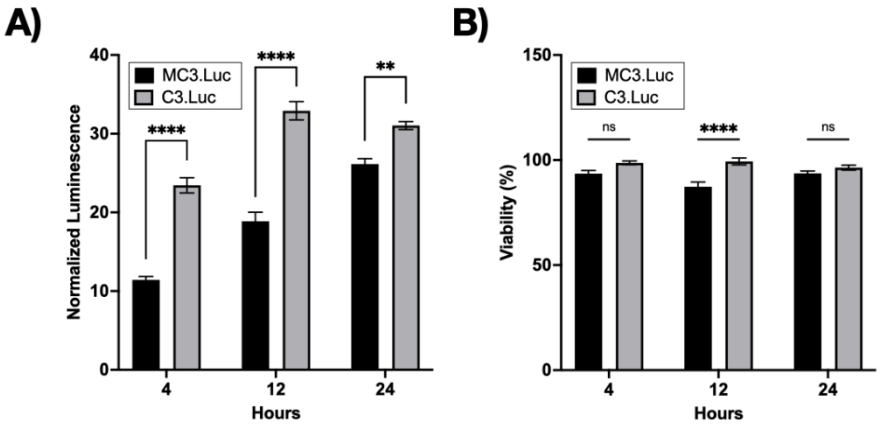

Fig. S1 | Luciferase expression (A) and viability (B) of Neuro-2A cells after treatment with either C3 or MC3 LNP (100 ng of mRNA) encapsulating luciferase mRNA. ** $p < 0.01$, **** $p < 0.0001$ by two-way analysis of variance (ANOVA) with post-hoc Šídák's multiple comparisons test.

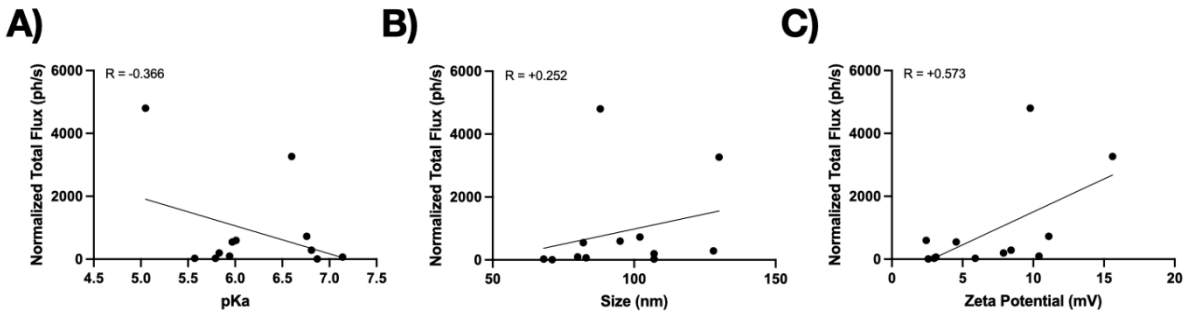

Fig. S2 | Relationship between LNP library physiochemical properties – including (A) pK_a, (B) size, and (C) zeta potential – and LNP transfection efficacy *in vivo* after ICV injection to E18 Balb/c fetuses as measured by quantification of luciferase signal 4 hours after administration via IVIS imaging. Correlation coefficient (R) of linear regression analysis is reported in the top left corner of each individual graph.

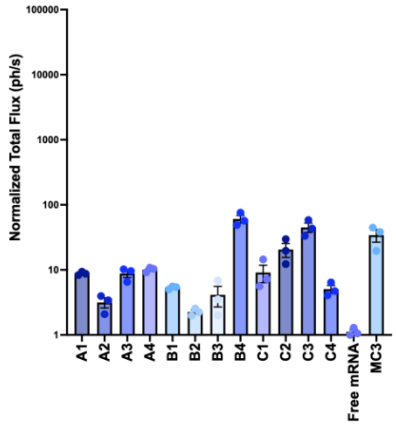

Fig. S3 | Quantification of *luciferase* signal via IVIS imaging from harvested livers of E18 BALB/c fetuses 4 hours after ICV injection (1 mg/kg) with each LNP in the screening library, free mRNA, or MC3 LNP following normalization to background autofluorescence.

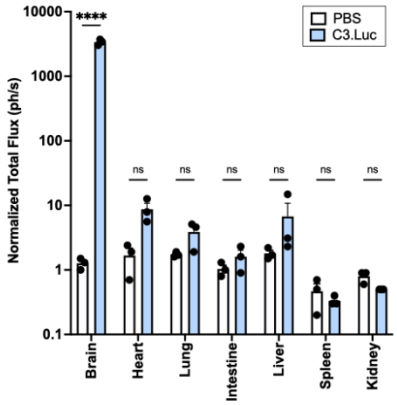

Fig. S4 | Quantification of *luciferase* signal via IVIS imaging from harvested organs (brain, heart, lung, intestine, liver, spleen, kidney) of E18 BALB/c fetuses 4 hours after ICV injection (1 mg/kg) with C3 LNP or PBS following normalization to background autofluorescence. **** $p < 0.0001$ by two-way analysis of variance (ANOVA) with post-hoc Šídák's multiple comparisons test.

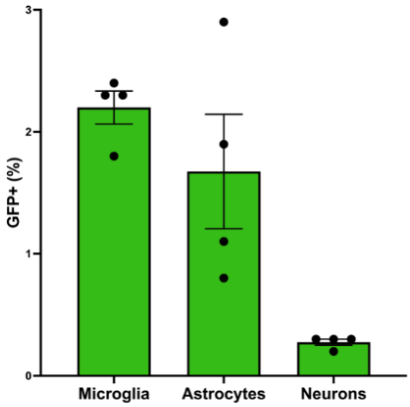

Fig. S5 | Percentage of green fluorescent protein (GFP) positive cells among sub-populations of microglia ($CD11b^{+}/CD45^{lo}$), astrocytes ($GFAP^{+}/CD45^{-}$), and neurons ($NFM^{+}/CD45^{-}$) in the brain after ICV injection (1 mg/kg) of C3 LNPs encapsulating Cre mRNA to P0 $R26^{mTmG}$ neonates.

LEVELS	FACTORS (MOLAR RATIO %)		
	Ionizable Lipid	DOPE	Cholesterol
1	29	13	40
2	35	16	46.5
3	41	19	53

Fig. S6 | Orthogonal DOE array displaying the range of excipient molar ratios used in C3.1-C3.9 LNP formulation.

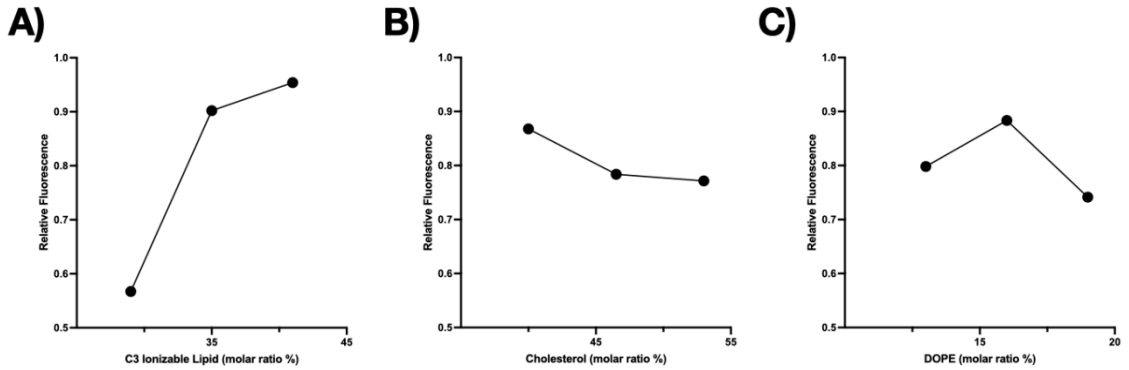

Fig. S7 | Impact trend curves generated during design-of-experiments investigation for C3 ionizable lipid, DOPE, and cholesterol, respectively, on *in vitro* LNP-mediated mRNA transfection efficacy in Neuro-2A cells.

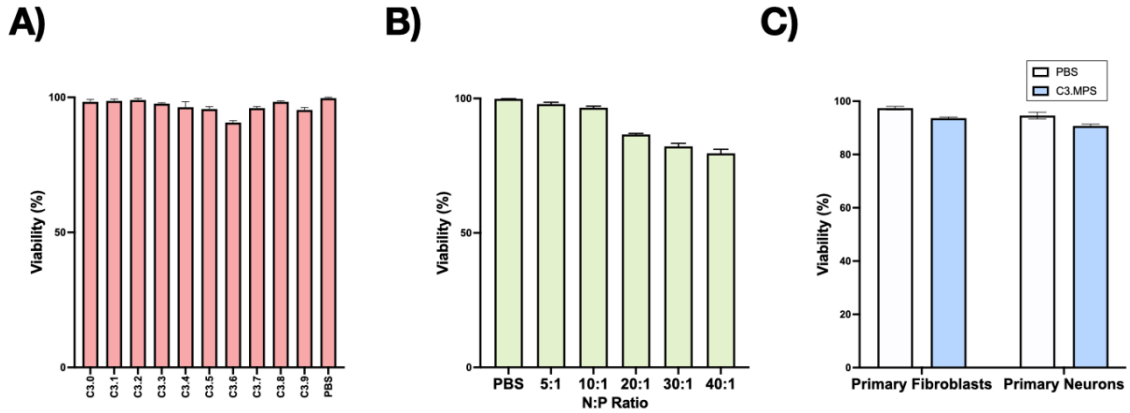

Fig. S8 | Viability after treatment by C3 LNPs (200 ng of mRNA) with different excipient ratios (A) or different N:P ratios (B) in Neuro-2A cells and after treatment by C3.MPS LNPs (200 ng of total mRNA) in primary fibroblasts / primary neurons isolated from an *IDUA*-W392X mouse (C)

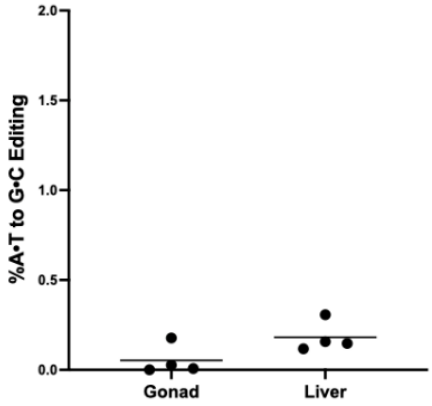

Fig. S9 | Next-generation sequencing data of DNA isolated from the liver and gonadal tissue of C3.MPS LNP treated *Idua*-W392X neonates at the target G→A *Idua* site, normalized to data collected from PBS-injected negative control animals.

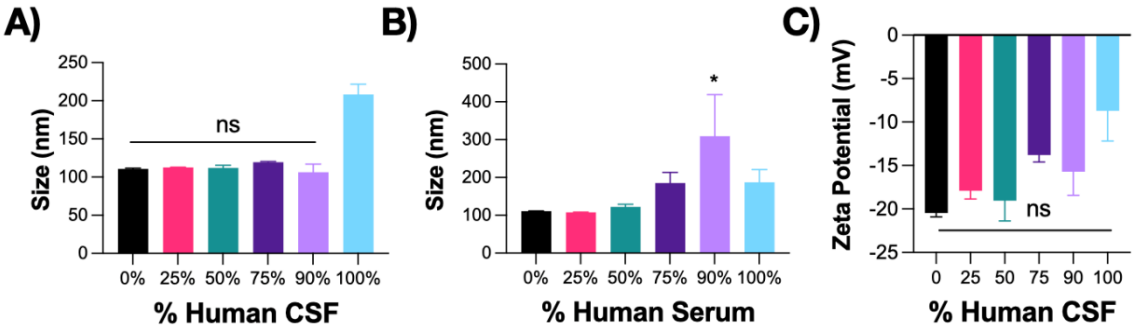

Fig. S10 | Size and PDI measurements of C3.MPS LNPs incubated in either human cerebrospinal fluid (A) or human serum (B) at increasing volume percentages of biological fluid, along with zeta potential measurement of C3.MPS LNPs incubated in increasing volume percentages of human cerebrospinal fluid (C). **** $p < 0.0001$ by one-way ANOVA with post-hoc Dunnett's test compared to positive control (0%).